ISSN: 2350-0328
International Journal of Advanced Research in Science, Engineering and Technology
Vol. 10, Issue 5, May 2023

Dynamic Properties and Stability Limits of Machine Tool Spindle and Cutting Tool Assembly

Egamberdiyev Ilkhom Pulatovich, Ochilov Ulugbek Yunusovich, Irnaeya Lutfiya Saloyiddin kizi

DSc, professor, Navoi State Mining and Technologies University, Navoi, Uzbekistan
Assistant, Navoi State Mining and Technologies University, Navoi, Uzbekistan
Master's degree student, Navoi State Mining and Technologies University, Navoi, Uzbekistan

ABSTRACT: The manufacturing industry is facing intense competition, prompting the exploration of efficient cutting operations to minimize costs. Enhanced productivity necessitates faster machining and reduced cycle times, resulting in a desire to increase process parameters such as cutting speed, feed velocity, and depth of cut. This study employs a rational combination of experimental and analytical modeling to characterize the dynamic properties of the system. This approach has the potential to expedite cutting tool development and cutting process planning, ultimately saving time and costs. The project's primary objective is to characterize the dynamic properties of the interface between the machine tool spindle and cutting tool in a machine tool/cutting tool assembly. Establishing a model description that is suitable for further analysis is a priority. Information regarding the spindle interface, coupled with finite element (FE) analysis of the cutting tool, will provide the necessary details for determining the optimal design and cutting data to avoid regenerative vibrations. It will also enable the prediction of tool tip response under time-varying loads. The goal is to maximize productivity, process stability, and reliability, while minimizing dynamic testing.

KEY WORDS: stability, mechanical components, vector, milling model, capability, productivity.

I. INTRODUCTION

The stability limit refers to the point at which the cutting process becomes unstable, resulting in chatter vibrations. The theoretical framework presented in [4] and [5] for turning operations was later extended by Budak and Altintas [6, 7] to be applicable for milling as well. They introduced a dynamic milling model with directional dynamic milling force coefficients, which enabled an analytical solution that better considered the change in direction of the cutting force in a milling operation. The analytical solution to the stability problem presented in [4–7] can be established based on raw frequency response function (FRF) data directly, and no system model identification is required. However, this solution assumes a linear dependency between cutting forces and feed and depth of cut, which is not always accurate in practice. Non-linear dependencies, such as cutting tool jumping in and out of cut during vibrations and relations between cutting force and chip thickness, can alter the stability limit in ways that cannot be explained by the analytical solution. To address this issue, researchers have proposed time domain stability charts, which require a system model and are more time-consuming to establish. Budak and Altintas further advanced the theoretical framework for turning operations to include milling operations. They introduced a dynamic milling model that incorporates directional dynamic milling force coefficients. This model enables an analytical solution that accounts for changes in cutting force direction during milling operations. The resulting stability lobe charts provide a graphical representation of the stability limit as a function of spindle speed and depth of cut.

Unlike other stability analysis methods that require system model identification, the analytical solution presented in [6, 7] can be established directly from raw frequency response function (FRF) data. However, this approach assumes that the cutting forces have a linear dependency with respect to feed and depth of cut. This approximation is not always accurate, and non-linear dependencies such as cutting tool jumping or non-linear relations between cutting force and chip thickness can alter the stability limit in ways that cannot be explained by the analytical solution. An alternative approach to the analytical solution presented earlier is the use of a time domain stability chart, as discussed in references [8]. This method allows for a non-linear solution of machining stability but requires a system model and is more time-consuming to establish [13-17].

ISSN: 2350-0328
International Journal of Advanced Research in Science, Engineering and Technology
Vol. 10, Issue 5, May 2023

First principal modelling approaches are commonly used for dynamic analysis of mechanical components. However, the machine tool is a complex mechanical structure with multi-axial motion capabilities, as shown in Figure 1. It is assembled with numerous mechanical joints to enable such complex motion, making it difficult to model using a finite element model (FEM) approach. The dynamic properties at the interface of cutting tools are also difficult to predict, rendering such approaches insufficiently accurate in predicting the tool tip frequency response of the machine tool/cutting tool assembly. The most common method for obtaining the required frequency response functions (FRFs) at the tool tip is through experimental dynamic testing. The advantage of this approach is that the system flexibility and damping are embedded in the measured FRF, thus accounting for them. However, the experimental approach also has its challenges. For instance, in the case of optimizing a multi-operational machine tool, this approach requires physical testing of a multitude of machine-tool/cutting tool combinations. Furthermore, the dynamic properties change with the variation in geometric properties of the different cutting tools, necessitating separate establishment of FRFs for each cutting tool of interest. Additionally, the machine tool needs to be taken out of operation during measurements, resulting in the loss of valuable production time.

To reduce measurement time, a technique called sub structuring can be employed to synthesize the dynamic response at the tool tip, as discussed in references. This technique treats the machine tool as an assembly of subsystems, allowing the frequency response to be obtained through sub structuring based on a combination of measurements, modeling, and analysis depending on what best suits the substructure in question. The dynamic characteristics of the machine tool are preferably obtained experimentally, while the less complex cutting tool can be modeled using first principle analytical beam models or finite elements.

II. MODELS IN STRUCTURAL DYNAMICS

Mathematical models that illustrate structural components are crucial in parts making as they allow for the evaluation and selection of product concepts at an early stage, before physical prototypes are produced and experimental testing begins. First principal modeling, based on fundamental laws of physics of Newton's and Hook's laws, is often the mostly used modeling types. This approach enables analysis of deflection, stress, and strain responses as the model is subjected to assigned load cases. The complexity of the model typically increases as the concept matures, starting with simplistic analytical beam models, which may be sufficient for early-stage evaluations, and progressing to more complex finite element (FE) models, as demonstrated by Sabye and Peterson [11].

Dynamic structural analysis of linear discrete physical models is commonly performed using a second-order ordinary differential equation (ODE) formulation, as outlined by Craig and Kurdila [12]. This formulation relates the nodal displacement vector {q} ∈ R m, where m represents the number of degrees-of-freedom (DOF) in the system, to the load vector {f} using symmetric mass matrix M, viscous damping matrix V, and stiffness matrix K, as shown in the following equation:

$$M\{\ddot{q}(t)\} + V\{\dot{q}(t)\} + K\{q(t)\} = \{f(t)\} \quad (1)$$

As f is associated with the applied load at each DOF the load vector can preferably be rewritten using a matrix P_u to relate the applied stimuli vector, {u} ∈ R^p where p denotes the number of inputs, to a subset of DOFs

$$\{f(t)\} = P_u \{u(t)\} \quad (2)$$

Similarly, it is also possible to selectively establish the displacement output, {y} ∈ R^r where r denotes the number of outputs, at a desired set of DOFs using

$$\{y(t)\} = P_d \{q(t)\} \quad (3)$$

Provided that the mass matrix is non-singular, hence invertible, the second order formulation, Equation (1), lends itself to a reformulation into first order form known as state-space form

$$\begin{cases} \{\dot{x}(t) = A\{x(t) + B\{u(t)\}\} \\ \{y(t)\} = C\{x(t)\} + D\{u(t)\} \end{cases} \quad (4)$$

here $\dot{x}(t)$ is the n-dimensional state vector where n = 2m. The constant coefficient matrices quadruple {A, B, C, D}, holds the state matrix A ∈ $R^{n\times n}$, the input matrix B ∈ $R^{n\times p}$, the output matrix C ∈ $R^{r\times n}$ and the feed-through matrix D ∈ $R^{r\times p}$.

This structure is often preferred in control theory but is also very suitable in system identification of experimentally obtained model descriptions. The second order equation is cast in a first order form by introduction of the state vector

$$\{x(t)\} = \begin{Bmatrix} \{q(t)\} \\ \{\dot{q}(t)\} \end{Bmatrix} \quad (5)$$

ISSN: 2350-0328
International Journal of Advanced Research in Science, Engineering and Technology
Vol. 10, Issue 5, May 2023

and after some manipulation of Equation (1) with the extension of Equation (2) and introduction of the dummy equation $\{\dot{q}(t)\} = \{\dot{q}(t)\}$, the state coefficient matrices in Equation (4) are made to relate to the second order form as

$$A = \begin{bmatrix} 0 & I \\ -M^{-1}K & -M^{-1}V \end{bmatrix}, B = \begin{bmatrix} 0 \\ M^{-1}P_u \end{bmatrix}, C = \begin{bmatrix} P_d & 0 \\ 0 & P_v \end{bmatrix} \quad (6)$$

where subscripts d and v relate to displacement and velocity respectively. The output equation, for selected displacements, y_d, and velocities, y_v, is

$$\{y(t)\} = \begin{Bmatrix} \{y_d(t)\} \\ \{y_v(t)\} \end{Bmatrix} = \begin{bmatrix} P_d & 0 \\ 0 & P_v \end{bmatrix} \{x(t)\} \quad (7)$$

As stated, the state vector includes both displacement and velocity outputs, so the feed-through matrix D is only used when the state-space model output is acceleration. Since acceleration is a component of $\dot{x}(t)$, the equation for the selected acceleration output, y_a, can be obtained by using dynamic Equation (4) as follows:

$$\{y_a(t)\} = [0 \quad P_v]A\{x(t)\} + [0 \quad P_v]B\{u(t)\} \quad (8)$$

which gives the direct throughput matrix for accelerations being $D = [0 \quad P_v]B$.

III. TIME-DOMAIN MODEL

The time-domain model takes into account the regenerative effect caused by the interaction between the tool and the workpiece. The dynamic deflection of the tool is also considered in the model, which is important for accurately predicting the machining stability. The model simulates the dynamic chip thickness, cutting forces, and tool displacements at discrete time steps during the milling process. This allows for prediction of the behavior of the system, including the oscillatory nature of the chip thickness and resulting changes in cutting forces and tool displacements. By accurately modeling these dynamic effects, the time-domain model provides valuable insight into the machining stability and helps to optimize the milling process.

Dynamic chip thickness

The amplitude of the dynamic chip thickness is influenced by the feed per tooth and the vibrations during the current and preceding tooth periods. The milling tool is modeled to have two degrees of freedom, namely the feed direction (X) and the normal direction (Y). When the cutting forces excite the tool in these directions, dynamic displacements are calculated for each degree of freedom at a specific time.

$$v_j = -x \cdot \sin\phi_j - y\cos\phi_j \quad (9)$$

The displacement magnitude in the feed direction is denoted by x while the displacement magnitude in the normal direction is denoted by y. Additionally, the instantaneous angular immersion ϕ_j is a function of time, with $\phi_j = sp \cdot t$; representing the spindle speed in rpm. The equation describing the dynamic chip thickness is given by:

$$h(t) = f_t \cdot \sin\phi_j \cdot \sin k + v_{j,0}(t-\tau) - v_j(t) \quad (10)$$

Where the tooth period (τ) is defined as $\tau = 60 / (sp \cdot N)$; and $v_j, v_{j,0}$,0 are the dynamic displacements of the cutting tool at the present and previous tooth periods, respectively.

Dynamic displacements

The calculation of dynamic displacement involves modeling the tool as a system that comprises of masses with a single degree of freedom in the X and Y directions. The movement in the X and Y directions is expressed by:

$$m_x\ddot{x} + c_x\dot{x} + k_x x = F_x \quad (11)$$
$$m_y\ddot{y} + c_y\dot{y} + k_y y = F_y$$

In order to compute the accelerations in both the X and Y directions at the current time step, the equation of motion is used. Specifically, the current acceleration is derived from the previous time step's velocities and positions. For the initial time step, velocities and positions are set to zero. Numerical integration via Euler's method is then used to determine the present positions. Finally, the dynamic cutting forces are computed using Equation 5, but with the dynamic chip thickness substituted in place of the static chip thickness.

Verification of the force models

The validity of the force model was tested by conducting a cutting force experiment using two indexable tools. The first tool consisted of 4 negative round ceramic inserts and the second tool consisted of 5 positive round ceramic inserts, both with a diameter of 63 mm and inserts of 12.7 mm diameter. The first tool had an axial rake angle of -7° and a radial rake angle of -13°, while the second tool had a radial rake angle of -3° and 0 axial rake angle. The experiment was performed on a NF-630 machine, using Cr12N18 as the workpiece material, and slot milling with an axial depth of 0.5 mm. The spindle speeds used were 800, 850, and 900 rpm, and the feed rate was varied at each spindle speed, with values of 0.0465, 0.0775, 0.0969, and 0.1162 mm/tooth. A total of 12 tests were conducted for each cutting tool, and the cutting forces were measured using a Kistler 9255B dynamometer.

ISSN: 2350-0328
International Journal of Advanced Research in Science, Engineering and Technology
Vol. 10, Issue 5, May 2023

The CFCs (Coefficient of Frictional Forces) were estimated using a Matlab® algorithm that was implemented in a graphical user interface (GUI). An example of the calculated CFCs at a rotational speed of 1100 rpm. It is observed that for large negative rake angles, the CFCs can be considerably higher than K_{rc}, as seen for the first tool. The GUI also integrated static and dynamic cutting force models to predict the cutting forces, which were then compared with the experimental data. As a run-out effect was observed in the measured cutting forces in some of the tests, the static force model was modified to include the uneven distribution of feed rate among the inserts to improve the agreement with the experimental cutting forces.

The figures presented in the study show a representative comparison of cutting forces for each tool type. In Fig. 10(a), the cutting forces for Tool 1 are plotted for one tool revolution, and no run-out effect is observed. In contrast, Fig. 10(b) shows the cutting forces for Tool 2, and the run-out effect is clearly visible, leading to uneven force contributions among the teeth. The static force model was modified to account for the run-out effect for Tool 2, resulting in better agreement with the measured cutting forces. However, the dynamic force model did not account for the run-out effect, leading to a slight discrepancy between the static and dynamic cutting force predictions for some teeth.

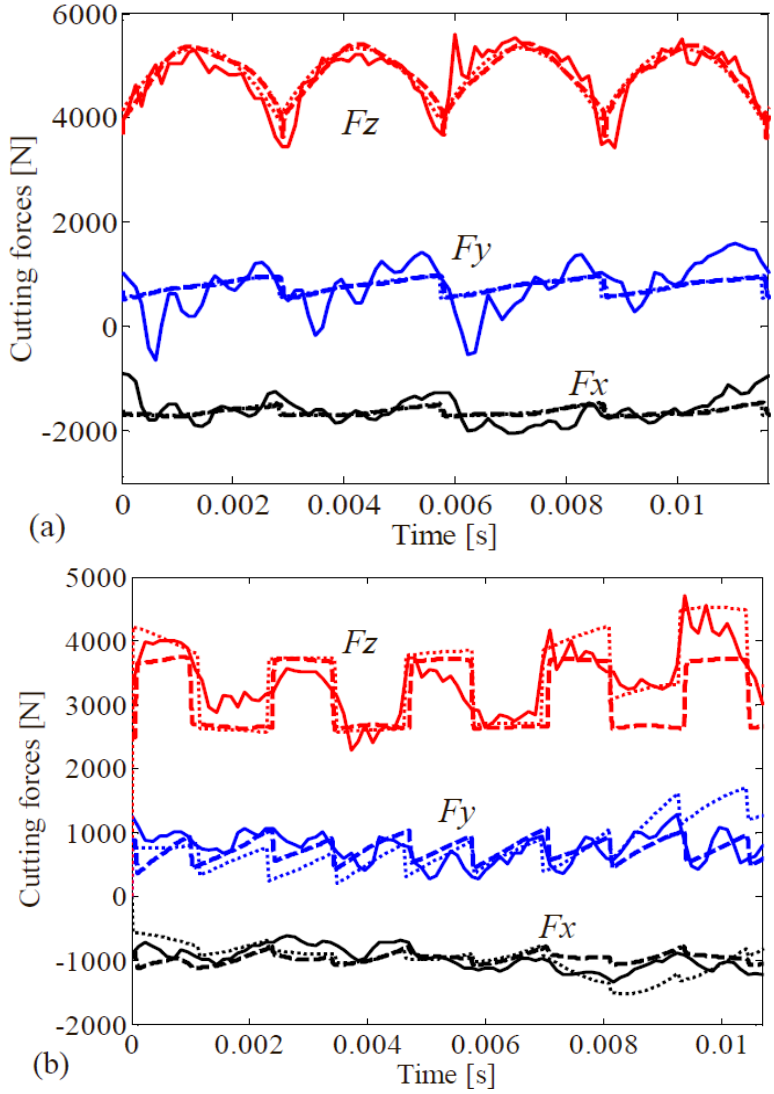

Fig. 1. Comparison of measured cutting forces (solid line), simulated static cutting forces (dotted line) and simulated dynamic cutting forces (dashed line), 100% radial immersion, *sp* =519 rpm, *ft* = 0.116 mm/tooth. a) First tool. b) Second tool.

ISSN: 2350-0328
International Journal of Advanced Research in Science, Engineering and Technology
Vol. 10, Issue 5, May 2023

Based on the simulations, it was concluded that the experimental cutting tests were performed under stable conditions, as the dynamic component of the chip thickness was not significant. As a result, the simulated dynamic cutting forces were very similar to those obtained using the rigid tool model. The cutting forces of the first tool were about 45% higher in the X-direction, 35% higher in the Y-direction, and 75% higher in the Z-direction compared to the second tool, due to the different insert orientation angles. Although there were more variations in cutting force for the second tool, there was still good agreement between the measured and predicted forces for both cases.

IV. STABILITY ANALYSIS

A time-domain model was used to set some operating conditions and find stability limits to sketch the stability lobes. Table 1 shows the estimated maximum axial depth of cut that ensures a stable milling process for the experimental spindle speeds. The CFCs were averaged for the spindle speeds under analysis to estimate the stability lobes, which are shown in Figures 12 and 13. The second tool had higher stability limits and lower cutting forces than the first tool, which may be due to the lower force magnitudes observed in the second tool.

Table 1. Stability limits

Spindle speed (rpm)	Axial cutting stability limit (mm) Tool 1	Tool 2
800	6.3	4.7
1000	3.4	2.1
1200	1.7	3.7

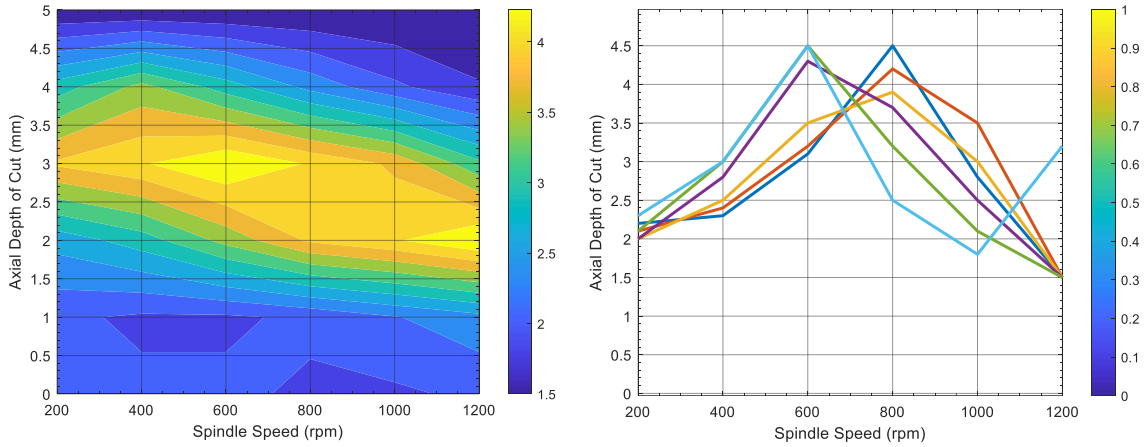

Fig. 2. Stability limits.

V. CONCLUSION

The article presents cutting force models for indexable tools with round inserts. The models were experimentally verified, and the results showed reasonable accuracy. Stability limits were predicted for both tools, and future work will verify these predictions with additional cutting tests. The developed models can be used to optimize cutting parameters for different tool configurations, reducing time and costs of cutting trials.

REFERENCES

[1]. Altintas Y., Budak. E., 1995 Analytical Prediction of Stability Lobes in Milling. CIRP Annals - Manufacturing Technology, 44:357-362.
[2]. Fu H.J., Devor R. E., Kappor S.G. 1, 1984, A Mechanistic Model for the Prediction of the Force System in Face Milling Operations, ASME Journal of Engineering for Industry, 106:81-85.
[3]. Engin S. and Altintas Y. 2001, Mechanics and Dynamics of General Milling Cutters. Part II: Inserted Cutters, International Journal of Machine Tools and Manufacture, 41: 2213-2231.
[4]. Altintas Y., Kilic Z., Kaymakci M. 2012, Unified Cutting Force Model for Turning, Boring, Drilling and Milling Operations, International Journal of Machine Tools and Manufacture, 54-55: 34-45.
[5]. Kim S.J., Lee H.-U., Cho D. 12-13, 2006, Feed Rate Scheduling for Indexable End Milling Process Based on an Improved Cutting Force Model, International Journal of Machine Tools and Manufacture, Vol. 46:1589-1597.

ISSN: 2350-0328
International Journal of Advanced Research in Science, Engineering and Technology
Vol. 10, Issue 5, May 2023

[6]. Liu Z. Q., Cao. C. M., Du J., Shi Z. Y. 2012, Effect of Cutting Speed on Surface Integrity in High Speed Machining Nickel-Based Superalloy Inconel 718. 697, 208–212.
[7]. Yusuf Altintas, 2000, Manufacturing Automation Metal Cutting Mechanics, Machine Tool Vibrations, and CNC Design, Cambridge University Press.
[8]. Gradisek K., Kalveram J., Weinert M. 2013, Mechanistic Identification of Specific Force Coefficients for a General End Mill. International Journal of Machine Tools & Manufacture, 44:401-414.
[9]. Ozturk E, Taylor C. M., Turner S. and Devey M, 2011, Modelling and Development of a High Performance Milling Process with Monolithic Cutting Tools, AIP Conf. 1353:663- 668.
[10]. Schmitz T. L., Smith K S., 2008, Machining Dynamics: Frequency Response to Improved Productivity. Springer.
[11]. N. Saabye and H. Petersson. Introduction to the Finite Element Method. Prentice Hall Internationa, 1992.
[12]. W.K. Gawronski. Dynamics and control of structures: a modal approach. Springer, New York, 1998.
[13]. Egamberdiev I.P. Spectral analysis of the oscillatory process of support assemblies on drilling machines // International Journal of Advanced Research in Science, Engineering and Technology. – National Institute of Science Communication and Information Resources– India, 2018. –Vol. 5. – Issue 5. – pp. 5958-5962.
[14]. Egamberdiev I.P., Atakulov L., Muminov R.O., Ashurov Kh.Kh. Research of Vibration Processes of Bearing Units of Mining Equipment // International Journal of Advanced Trends in Computer Science and Engineering. – Volume 9, No.5, September - October 2020. – pp.7789-7793 (Scopus Base, DOI: 10.30534/ijatcse/2020/125952020).
[15]. Muminov R.O., Egamberdiev I.P., Ashurov Kh.Kh., Makhmudova M.F. Experimental Studies of the SBSH-250MNA-32 Mining Drilling Rig. International Journal of Advanced Research in Science, Engineering and Technology Vol. 8, Issue 11 , November 2021. Copyright to IJARSET www.ijarset.com 18637-18644. (05.00.00; №8).
[16]. Sh.N. Yaxshiyev, Kh.Kh. Ashurov, A.J.Mamadiyarov Dynamics of Spindle Assembly of Metal-Cutting Machine // International Journal of Engineering and Advanced Technology (IJEAT) ISSN: 2249 – 8958, Volume-9 Issue-3, February 2020. 3121-3125.
[17]. Egamberdiev I.P., Mirzaev A.U., Zoirov Sh.Sh., Yaxshiev Sh.N. Razrabotka metoda monitoringa texnicheskogo sostoyaniya opornых uzlov gornogo oborudovaniya // Ilm-fan va innovatsion rivojlanish. – Toshkent, 2020. – №1.– S. 114-119.